Available online at www.sciencedirect.com
SCIENCE DIRECT®
Journal of Solid State Chemistry 178 (2005) 694–701
JOURNAL OF SOLID STATE CHEMISTRY
www.elsevier.com/locate/jssc

Hydrothermal reversible interconversion of two zincophosphates with three-dimensional open frameworks containing diprotonated 1,4-diazacycloheptane molecules

Michael Wiebcke[a,*], Clemens Kühn[a], Gerhard Wildermuth[b]

[a]*Institut für Anorganische Chemie, Universität Hannover, Callinstrasse 9, D-30167 Hannover, Germany*
[b]*Universität Konstanz, Fachbereich Chemie, D-78457 Konstanz, Germany*

Received 29 October 2004; received in revised form 17 December 2004; accepted 17 December 2004

Abstract

A new zincophosphate (ZnPO), $(C_5H_{14}N_2)[Zn_2(HPO_4)_3]$ (**I**), has been synthesized in the presence of 1,4-diazacycloheptane under mild hydrothermal conditions (160 °C) and the crystal structure determined by single-crystal X-ray crystallography. Corner-sharing ZnO_4 and HPO_4 tetrahedra are arranged into layers that are based on the 2D, three-connected 4.8^2 net and linked together by tetrahedral HPO_4 pillars into the 3D interrupted open framework. The 3D intersecting channel system is filled with diprotonated amine molecules. It has been observed that **I** forms via hydrothermal transformation of a known ZnPO hydrate, $(C_5H_{14}N_2)[Zn_2(HPO_4)_3]\cdot H_2O$ (**II**), with a closely related 3D open-framework structure, involving dehydration and reconstruction of Zn–O–P linkages. Interestingly, this transformation is completely reversible under hydrothermal conditions at temperatures between 100 and 160 °C with **II** and **I** being stable at low and high temperature, respectively. Also, **I** and **II** can be interconverted via solid–gas reactions. Crystal data for **I**: Orthorhombic, space group $Pca2_1$, $Z = 16$, $a = 14.6595(9)$, $b = 14.557(1)$, $c = 28.114(2)$ Å, $T = 298$ K.

Keywords: Zincophosphate; 1,4-diazacycloheptane; Crystal structure; Phase transformation; Hydrothermal synthesis

1. Introduction

Since the first syntheses of zincophosphates (ZnPOs) with zeolite tetrahedral frameworks [1] in 1991 by Stucky and coworkers [2,3], a large number of new ZnPOs has been reported [4,5], as a result of the interest in new microporous materials with potential applications, e.g., in catalysis, separation and as advanced host–guest systems [6–8]. ZnPOs can be prepared under particularly mild conditions (even below ambient temperature [2]) and frequently in the form of single crystals. The materials synthesized in the presence of alkali metal cations, organic amines and, more recently, transition-metal complexes [9] possess 0D, 1D, 2D and 3D ZnPO partial structures which are mainly built from corner-linked ZnO_4 and PO_4 tetrahedra, but ZnO_5 and ZnO_6 units and coordination of N-donor ligands to the Zn^{2+} centers are also encountered. However, even 3D open-framework ZnPOs have generally low thermal stability. Notable exceptions are some members of the family of phases $M_3[Zn_4O(XO_4)_3]\cdot nH_2O$ (M = univalent cation; X = P, As) [10] which contain OZn_4 groupings in the framework and are structurally related [11] to the famous *M*OF-5-based series of isoreticular metal-organic framework solids with extra-large pores [12].

Of particular importance with regard to a more rational synthesis of microporous materials is an improved understanding of the mechanisms of phase formation on a molecular scale [13]. Because of the huge body of structural information now available for

*Corresponding author. Fax: +49 511 762 3006.
E-mail address: michael.wiebcke@acb.uni-hannover.de (M. Wiebcke).

0022-4596/$ - see front matter © 2005 Elsevier Inc. All rights reserved.
doi:10.1016/j.jssc.2004.12.026

ZnPOs, these systems appear to be well suited for studies in those directions. Following original hypotheses based on the assembly of 0D secondary building units introduced by Férey [14] and on the rearrangement and assembly of a specific chain introduced by Ozin and coworkers [15], Rao et al. have proposed an *aufbau* model to explain the building up of 3D ZnPO structures from specific 0D oligomeric (single four-membered ring, S4R) and 1D chain species [16] and, accordingly, have carried out extensive ex situ studies on the transformation behavior of low-dimensional ZnPO phases under mild conditions [17–21]. First in situ synchrotron X-ray diffraction (XRD) studies have revealed that 3D ZnPO phases can crystallize directly from solution or via intermediate 1D and/or 2D crystalline phases [22–24]. However, experimental proof of specific precursors in solution is very difficult to obtain and for the ZnPO system still missing. By applying in situ solid-state ^{31}P NMR techniques, Natarajan et al. [25] have very recently obtained some more reliable evidence for the possible direct transformation of an S4R species into a 2D ZnPO phase. Interestingly, it has also been shown that 3D ZnPOs can be degradatively transformed into ZnPO phases of lower dimensionality by careful acid treatment [26]. Also, the acid degradation of 3D ZnPOs into hopeite, $Zn_3(PO_4)_2 \cdot 4H_2O$, has been investigated [27].

Here we report on the synthesis and crystal structure of a new 3D open-framework ZnPO, $(C_5H_{14}N_2)[Zn_2(HPO_4)_3]$ (**I**), with entrapped diprotonated 1,4-diazacycloheptane molecules. We show that **I** forms via hydrothermal transformation of a known ZnPO hydrate, $(C_5H_{14}N_2)[Zn_2(HPO_4)_3] \cdot H_2O$ (**II**), with a closely related 3D open-framework structure, involving dehydration and framework reconstruction. Interestingly, this transformation is completely reversible under hydrothermal conditions at temperatures between 100 and 160 °C with **II** and **I** being stable at low and high temperatures, respectively. We also show that **I** and **II** can be interconverted via solid–gas reactions. Methods employed were single-crystal X-ray crystallography, variable-temperature powder XRD and simultaneous thermogravimetric (TG) and difference thermal (DTA) analysis.

2. Experimental

2.1. Preparations and methods of characterization

Reagents used were 1,4-diazacycloheptane (homopiperazine, $C_5H_{12}N_2$), zink oxide, phosphoric acid (85 wt % in water) and deionized water. Hydrothermal reactions were carried out in home-made Teflon-lined stainless steel autoclaves with 8 mL capacity under static conditions and autogeneous pressure.

I was prepared from reaction mixtures of approximate molar compositions $1ZnO{:}2.2H_3PO_4{:}\ 13H_2O{:}\ 0.9C_5H_{12}N_2$. A typical experiment was as follows: A clear zinc phosphate solution was obtained by combining 2.26 g (85%) H_3PO_4, 2.10 g H_2O and 0.72 g ZnO. Under continuous stirring, 0.77 g solid amine was added in small portions. After addition of 2/3 of the total amount of amine a white suspension formed. The suspension was filled in an autoclave (degree of filling 40%) and kept at 160 °C for 2 days. The solid product was separated by filtration, washed with water and dried in air at 70 °C. No change of pH (ca. 4) was measured after hydrothermal treatment. The product consisted exclusively of large colorless, mostly rod-shaped crystals of **I** (maximum length ca. 0.3 mm). The yield was 60% (based on Zn). Elemental analysis, found/calc.: C, 11.52/11.53; H, 3.24/3.29; N, 5.36/5.38. Total TG weight loss, found/calc.: 29.6/27.8.

Large colorless crystals of **II** (various isometric polyhedral shapes, maximum size ca. 0.2 mm) were prepared under hydrothermal conditions (160 °C, 2 days) from reaction mixtures containing a higher amount of H_3PO_4 (approximate molar ratio $1ZnO{:}3H_3PO_4{:}24H_2O{:}1C_5H_{12}N_2$; pH ca. 2). Such mixtures did not yield **I**. Elemental analysis, found/calc.: C, 11.20/11.14; H, 3.21/3.55; N, 5.21/5.20. Total TG weight loss, found/calc.: 31.2/30.3.

Powder XRD patterns were measured at room temperature on a STOE STADI-P diffractometer in transmission mode using flat samples (Ge monochromator, Cu$K\alpha_1$ radiation, $\lambda = 1.54060$ Å, linear position-sensitive detector). For variable-temperature XRD studies the same instrument was equipped with a STOE heating attachment. Powdered solid samples were filled into thin-walled silica glass capillaries of 0.5 mm diameter which were left unsealed, i.e., open to air. Aqueous suspensions were filled into glass capillaries of 0.5 mm diameter which were sealed on both ends and fixed in a second glass capillary of 0.7 mm diameter. XRD patterns were recorded in Debye–Scherrer mode at various temperature steps. Heating and cooling rate between temperature steps was 5 °C/min. Each pattern was measured in 1 h between 8° and 36° 2Θ in the case of pure solids (measured from room temperature up to 400 °C) and between 11 and 30° 2Θ in the case of suspensions (measured between room temperature and 170 °C).

TG/DTA measurements were performed simultaneously on a Netzsch STA429 thermoanalyzer in a flow (160 mL/min) of pure oxygen up to 1030 °C with a heating rate of 5 °C/min.

2.2. Single-crystal X-ray structure analysis

Selected single crystals were glued to the tips of thin-walled glass capillaries and mounted on a STOE

IPDS image-plate diffractometer for the X-ray measurements (graphite monochromator, Mo$K\alpha$ radiation, $\lambda = 0.71073$ Å). Absorption corrections based on symmetry-equivalent reflections were applied (MULABS option in the PLATON package [28]). For structure solution (direct methods) and refinement (F^2 values, full-matrix least-squares method including all data), the programs SHELXS-86 [29] and SHELXL-97 [30] were used. The reflection conditions were consistent with the acentric space group $Pca2_1$ and the centric space group *Pbcm*. The structure was solved and refined in $Pca2_1$ as a racemic twin (twin fractions 0.633(8), 0.367(8)). A number of ZnPO framework and amine atoms were found to be positionally disordered. The disordered non-H atoms were refined with isotropic displacement parameters, while all remaining non-H atoms were refined anisotropically. H atoms of the diprotonated amine molecules were geometrically constructed and allowed to ride in idealized positions on the respective C and N atoms. Eight out of the total of 12 framework H atoms were located on difference Fourier maps. These H atoms were refined using a restraint for the O–H bond length (0.90(2) Å). The missing framework H atoms were not considered in the structure refinement. Restraints on bond distances (for C–C and C–N bonds) and isotropic displacement parameters of the disordered non-H atoms were still applied in the final cycles of refinement.

An ADDSYM analysis (PLATON [28]) revealed that the final structure model is pseudo-centrosymmetric and close to *Pbcn* (not *Pbcm*) space-group symmetry. This can be seen after transformation of the cell axes by 0 1 0/1 0 0/0 0 –1 and shift of origin by −0.251, −0.243, 0.464. The large number of weak reflections that violate the reflection conditions of the *n* glide plane, the acentric intensity distribution and the reasonable structure refinement indicate that $Pca2_1$ is the correct choice of space group. Structure determination was carried out on two different crystals of **I**. These analyses gave the same results, including twinning. The more precise structure analysis is presented here, details of which are summarized in Table 1. Crystallographic data have been deposited with the Cambridge Crystallographic Data Centre, 12 Union Road, Cambridge CB2 1EZ, UK as supplementary publication no. CCDC 258279.

3. Results

3.1. Formation and interconversion of I and II

Upon addition of 1,4-diazacycloheptane to a clear aqueous zinc phosphate solution at room temperature (see Experimental Section), compound **II** forms (fine white suspension). This is revealed by an XRD pattern taken from the solid immediately after complete addition of amine. The XRD pattern compares well with an XRD pattern simulated on the basis of crystal structure data (Fig. 1a). Hydrothermal treatment of the suspension at 160 °C results in complete transformation of **II** into **I**, as demonstrated by the XRD patterns shown in Fig. 1b. Interestingly, the transformation is reversible. Keeping the heterogeneous mixture of solid **I** and mother liquor in the autoclave at 100 °C overnight (17 h) leads to complete recrystallization of **II**; at room temperature this takes ca. 14 days. Variable-temperature XRD studies on a laboratory diffractometer (capillary technique) demonstrate that on heating the hydrothermal conversion of **II** into **I** proceeds on a time scale of about 1 h (time to record an XRD pattern). Fig. 2a displays a stack of selected XRD patterns. Only the patterns at 150 and 155 °C exhibit reflections of both **II** and **I**. It should be mentioned that the patterns of **I** are of very poor quality (bad signal-to-noise ratio) due to the considerable increase in crystal size during the transformation, indicative of solution-mediated processes. In the capillaries on the diffractometer reconversion of **I** into **II** could, however, not be observed at 100 °C within 17 h, possibly due to low crystal-to-liquid interfaces and low mass transport (formation of bubbles) in the small capillaries.

TG/DTA curves of **II** are displayed in Fig. 3, while selected XRD patterns of **II** recorded on the diffractometer at various temperature steps are displayed in Fig. 2b. Dehydration of **II** corresponds to the first endothermic event (DTA peak at 140 °C) with a sharp weight-loss step of 3.4% on the TG trace (calc. 3.3%).

Table 1
Crystal data and details of structure analysis for **I**, $(C_5H_{14}N_2)[Zn_2(HPO_4)_3]$

Empirical formula	$C_5H_{17}N_2O_{12}P_3Zn_2$
Formula weight	520.86
Crystal system	Orthorhombic
Space group; Z	$Pca2_1$; 16
a(Å)	14.6595(9)
b(Å)	14.557(1)
c(Å)	28.114(2)
V(Å^3)	5999.6(7)
T (K)	298
$\mu_{MoK\alpha}$ (mm^{-1})	3.586
ρ_{calc} (Mg m^{-3})	2.307
Crystal size (mm^3)	0.29 × 0.09 × 0.07
$2\Theta_{maxx}$ (deg)	52.20
Reflections measured	83299
Unique reflections (total); R_{int}	11814; 0.058
Unique reflections ($I > 2\sigma_I$)	9587
Refined parameters/restraints	864/23
$R1$[a] ($I > 2\sigma_I$)	0.030
wR_2[b] (all data)	0.063
Largest diff. peak/hole (e Å^{-3})	0.73/−0.58

[a] $R_1 = \Sigma(|F_{obs}|-|F_{calc}|)/\Sigma|F_{obs}|$.
[b] $wR_2 = [\Sigma w(F^2_{obs}-F^2_{calc})^2]/\Sigma[w(F^2_{obs})^2]^{0.5}$.

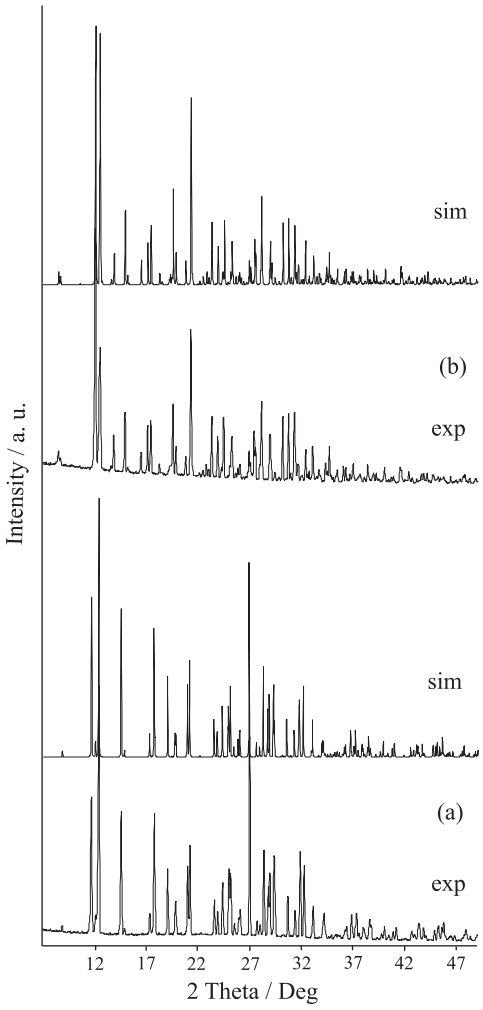

Fig. 1. Experimental and simulated XRD patterns (Cu$K\alpha_1$ radiation). (a) Compound **II**, and (b) compound **I**. An XRD pattern of **II** has been simulated on the basis of structure data taken from Ref. [5].

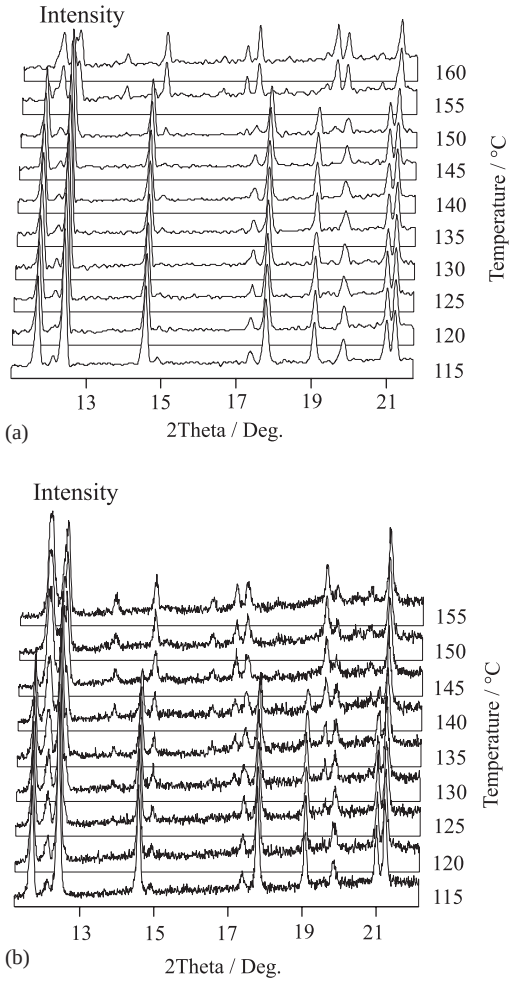

Fig. 2. Selected variable-temperature XRD patterns (Cu$K\alpha_1$ radiation). (a) Transformation of **II** into **I** under hydrothermal conditions (solid–liquid mixture in a sealed capillary), and (b) transformation of **II** into **I** in air atmosphere (pure solid in an open capillary).

On the XRD patterns, the transformation of **II** into **I** is seen to take place between 120 and 150 °C. On further heating, **I** decomposes at temperatures higher than ca. 290 °C in several endothermic and exothermic processes. First, the framework collapses and black amorphous material appears (XRD patterns from in situ studies up to 400 °C not shown). The loss of combustion products from the amine and water from framework hydroxyl groups and amine protons has completed at 820 °C, and the total weight loss amounts to 31.2% (calc. 30.3%). An XRD pattern taken from a sample of **II** after heat treatment in an oven at 830 °C for 17 h exhibits reflections of α-$Zn_2P_2O_7$ (ICDD database; card, 8-238).

In agreement with the observed large stability range on the TG curve (150–290 °C), **I** can be readily prepared by annealing solid **II** in air at 150 °C for 90 min. In wet atmosphere over concentrated $NaNO_2$ solution (66% humidity) at room temperature, ground samples of solid **I** adsorb water and slowly reconvert into **II** within ca. 8 weeks.

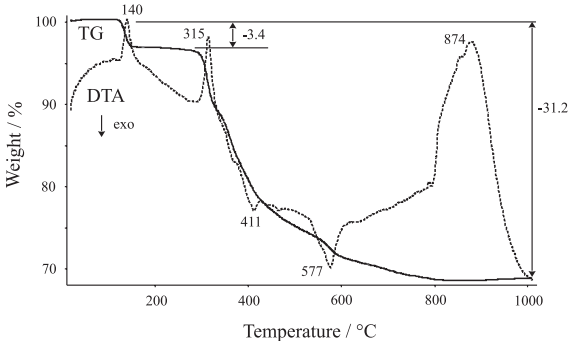

Fig. 3. TG/DTA curves of **II** measured under a flow of oxygen.

3.2. Crystal structure of *I*

An anionic 3D interrupted open framework, $^3_\infty[Zn_2(HPO_4)_3]^{2-}$, is generated by strictly alternating, corner-sharing ZnO_4 and HPO_4 tetrahedra. Within the inorganic framework, layers extending parallel (100)

may be identified (Fig. 4a) that are based on the 2D, three-connected 4.8^2 net (full vertex symbol 4.8.8) [31]. The Zn atoms of all ZnO_4 tetrahedra (atoms Zn1–Zn8) and the P atoms of 2/3 of the HPO_4 tetrahedra (atoms P1–P8) correspond to the nodes of net. The fourth corner of each tetrahedron protrudes up (U) or down (D) from the plane of a layer, and there are four distinct rings of four tetrahedra (four-membered rings, 4MR) with different orientations of the constituent polyhedra: Zn1–P8–Zn5–P1 (UDDU), Zn6–P5–Zn4–P6 (DDUD), Zn2–P4–Zn7–P2 (UUDU) and Zn8–P7–Zn3–P1 (UUDD). The fourth corner of the HPO_4 units represents a terminal OH group. The layers are stacked consecutively on top of each other (being transformed by the *c* glide planes) along the *a*-axis in ABAB fashion (Fig. 5) and are interconnected at the fourth corners of all ZnO_4 units through HPO_4 pillars (atoms P9–P12). Each pillar forms two Zn–O–P linkages and has in addition one P–OH and one P═O terminal function.

The thus-generated 3D framework is penetrated by different, intersecting channels running parallel to the three orthogonal cell axes. At the channel intersections reside the organic dications, some of which being disordered (Fig. 6). This can be understood when a detailed analysis of the system of pillars is made. There are principally two different ways of linkage by pillars with respect to the 4MR of adjacent layers, either "across" (a) or "vertical" (v) (see Fig. 5a and Fig. 6). Further, the v-pillars can be located "near to" (n) or "far from" (f) a given channel intersection (Fig. 6a). Thus, the void spaces at the channel intersections are not identical but fall into four distinct cages of different size and with different orientation of the P–OH and P═O functions of the pillars. As a result, the organic dications are more easily accommodated in the two cages having a- and vf-pillars than in the two cages having a- and vn-pillars. Additionally, one of the pillars (central atom P12) is orientationally two-fold disordered. As is displayed in Fig. 7, correlated with the orientation of the P12-centered tetrahedron are the H-atom positions at the hydroxyl O23 and O25 atoms (each being donor of a O–H···O bond) and the orientation of H_2N groups of two disordered organic dications (each being donor of N–H···O bonds). These disordered dications occupy the two distinct cages having a- and vn-pillars. As is typical for amine-containing interrupted framework ZnPOs, there exist extensive systems of guest–host N–H···O and intra-framework P–O–H···O hydrogen bonds.

The covalent bond lengths and angles in the ZnPO framework exhibit typical values, apart from two P–O distances involving disordered atoms which are slightly out of the typical range; Table 2 provides a brief survey. The donor and acceptor O atoms of the P–O–H···O

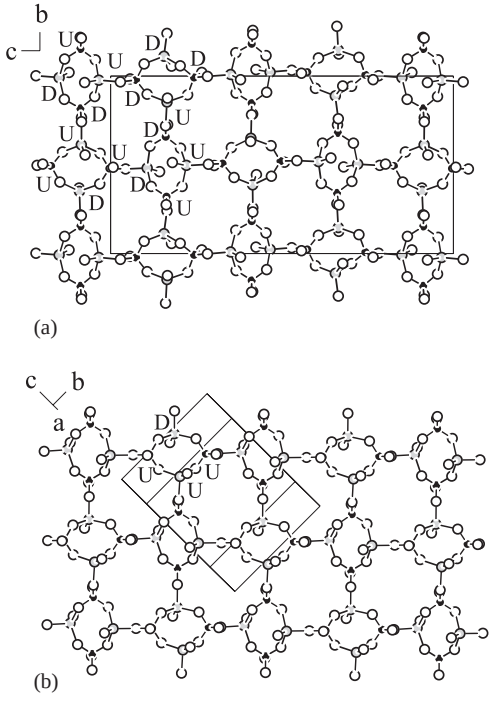

Fig. 4. (a) 2D, three-connected ZnPO layer of 4MRs and 8MRs in **I** (view is parallel to *a*-axis), and (b) in **II** (view is normal to the layer, i.e., along *a**-axis). Gray spheres, Zn atoms; black spheres, P atoms; white spheres, O atoms. Up (U) and down (D) orientations of the fourth corners of the ZnO_4 and HPO_4 units in distinct 4MRs are indicated. The drawing of **II** has been generated with structure data taken from Ref. [5].

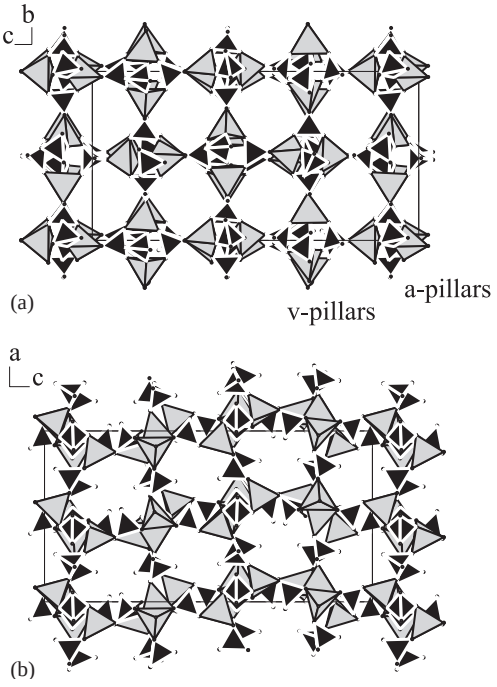

Fig. 5. 3D ZnPO framework of **I** in polyhedral representation as seen (a) normal to the 2D layers (along the *a*-axis), and (b) parallel to the 2D layers (along the *b*-axis). Grey tetrahedra, ZnO_4; black tetrahedra, HPO_4. The types of HPO_4 pillars are indicated (see text).

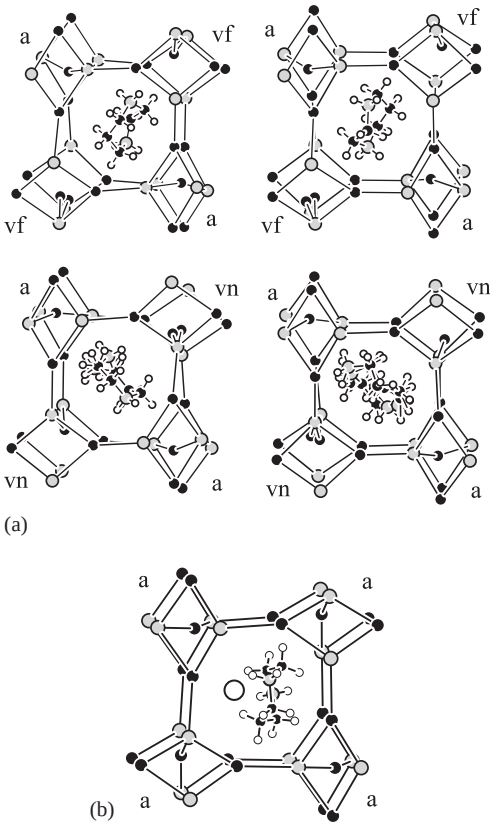

Fig. 6. (a) The four distinct cages (channel intersections) in **I** with the entrapped, partially disordered organic dications, and (b) the single distinct cage in **II** housing an ordered organic dication and a water molecule. ZnPO frameworks: Gray spheres, Zn atoms; black spheres, P atoms; O atoms omitted for clarity. Guest species: Gray spheres, N atoms; black spheres, C atoms; small white spheres, H atoms; large white sphere, O atom of water molecule. The types of HPO_4 pillars are indicated (see text); in **I** one of the pillars is two-fold disordered. The drawing of **II** has been generated with structure data taken from Ref. [5].

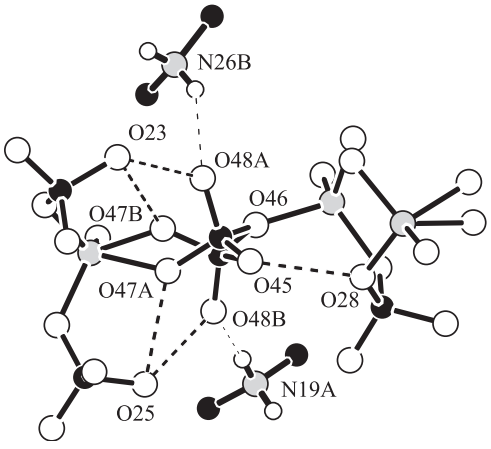

Fig. 7. Local details around a two-fold disordered P12-centered tetrahedral HPO_4 pillar. Atoms are shown as spheres of arbitrary radii. Hydrogen bonds are represented by dotted lines. The H atoms attached to O23, O25 and O45 have not been determined. Atom positions carrying an A or B label are statistically half occupied.

Table 2
Ranges of bond lengths (Å) and angles (deg) of the ZnPO framework for **I**, $(C_5H_{14}N_2)[Zn_2(HPO_4)_3]$

	Only ordered atoms participate	Disordered atoms participate
Zn–O	1.893(5)–1.969(4)	1.967(7)–1.967(8)
P–O	1.487(5)–1.601(4)	1.465(9)–1.669(5)
O–Zn–O	96.6(2)–121.7(2)	95.9(3)–123.2(3)
O–P–O	103.9(3)–113.7(3)	103.6(4)–117.1(5)
Zn–O–P	120.0(2)–145.4(3)	125.7(5)–146.6(4)

interactions have been derived on the basis of bond valence sum (VBS) calculations [32] and geometrical arguments. The VBS values for the P-bonded donor O atoms range from approximately 1.8–2.0 (estimates for contributions of O–H bonds have been derived from a graph (Fig. 2) in Ref. [32], and bond distances involving disordered atoms have been averaged). Eight out of the total of 12 H atoms (two being disordered) have been determined in the course of the structure analysis. The geometrical parameters of all O–H···O bonds are listed in Table 3. Included in Table 3 are the geometrical parameters for N–H···O bonds.

4. Discussion

The successful use of 1,4-diazacycloheptane as structure-directing agent in the synthesis of ZnPOs with 1D, 2D and 3D partial structures (including **II**) has been recently reported by Natarajan [5]. He used mixed organic–water solvent systems. The ready preparation of **II** in pure aqueous media and its various ways of reversible transformation into **I** are new findings.

To our knowledge, this is the first report of a thermally induced reversible interconversion of two different ZnPOs with 3D open frameworks in heterogeneous solid–solvent systems. For a better understanding of the reversible phase transformation, some additions to the recent structure description of **II** [5] are made here. The 3D ZnPO framework of **II** is closely related to the framework of **I** and possesses the same (4.8^2 net) layers and HPO_4 pillars. However, in **II** only one distinct 4MR with DUUU configuration occurs in the layers (Fig. 6b) which stack along the *a*-axis in AA fashion (the transformation of consecutive layers does not involve a mirror operation). Between adjacent layers there exist only a-pillars which link "across" 4MRs (Fig. 6b). The single distinct cage in **II**, being different from the cages in **I**, provides enough space and good orientation of P–OH and P=O groups to nice house and bind an ordered organic dication and an additional ordered H_2O molecule, the latter being located near an 8MR of a ZnPO layer (see Table 5 in Ref. [5] for guest–host interactions).

Table 3
Geometrical parameters of hydrogen bonds for **I**, $(C_5H_{14}N_2)[Zn_2(HPO_4)_3]$

Moiety	D–H (Å)	H···A (Å)	D···A (Å)	D–H···A (deg)
O20–H20···O32$^{\#1}$	0.88(2)	1.72(2)	2.586(6)	167(6)
O21–H21···O32	0.90(2)	1.67(2)	2.566(5)	174(7)
O23–H^a···O47B			2.72(1)	
O23–H^a···O48A			2.452(8)	
O25–H^a···O47A$^{\#7}$			2.776(9)	
O25–H^a···O48B$^{\#7}$			2.446(9)	
O27–H27···O24	0.89(2)	1.78(3)	2.642(6)	164(6)
O29–H29···O34$^{\#2}$	0.88(2)	2.21(3)	3.051(7)	159(7)
O30–H30···O37$^{\#3}$	0.90(2)	1.83(4)	2.640(6)	148(7)
O36–H36···O40$^{\#4}$	0.90(2)	1.58(2)	2.473(6)	176(7)
O39–H^a···O38$^{\#8}$			2.820(6)	
O41–H41···O8	0.88(2)	1.86(3)	2.712(5)	161(6)
O42–H42···O24$^{\#3}$	0.90(2)	1.72(2)	2.615(6)	177(7)
O45–H^a···O28$^{\#9}$			2.724(6)	
N4–H4A···O3	0.90	2.49	2.975(6)	114
N4–H4A···O34	0.90	2.41	3.210(7)	148
N4–H4B···O41$^{\#3}$	0.90	2.12	3.016(7)	175
N7–H7A···O7$^{\#3}$	0.90	2.07	2.946(6)	163
N7–H7B···O2$^{\#3}$	0.90	2.12	2.967(6)	156
N8–H8A···O5	0.90	2.59	3.162(7)	122
N8–H8A···O15	0.90	2.00	2.815(7)	150
N8–H8B···O39	0.90	2.27	3.158(8)	171
N12–H12A···O24$^{\#4}$	0.90	2.10	2.946(8)	155
N12–H12B···O17$^{\#4}$	0.90	2.15	3.007(8)	157
N12–H12B···O13$^{\#4}$	0.90	2.41	2.993(8)	122
N16A–H16A···O33$^{\#3}$	0.90	2.03	2.917(7)	170
N16A–H16B···O40$^{\#5}$	0.90	2.15	3.026(8)	165
N16A–H16B···O36$^{\#3}$	0.90	2.51	3.095(8)	123
N19A–H19A···O48B$^{\#6}$	0.90	1.84	2.74(1)	177
N19A–H19B···O31$^{\#1}$	0.90	2.00	2.89(1)	172
N19B–H19C···O31$^{\#1}$	0.90	2.09	2.97(1)	163
N19B–H19D···O26$^{\#5}$	0.90	2.26	3.15(1)	174
N23A–H23A···O4	0.90	2.40	3.15(1)	141
N23A–H23B···O10$^{\#3}$	0.90	2.07	2.96(1)	173
N23B–H23C···O10$^{\#3}$	0.90	1.93	2.76(1)	151
N23B–H23D···O4	0.90	2.01	2.91(1)	171
N26B–H26D···O48A$^{\#6}$	0.90	2.21	2.98(1)	143
N26A–H26A···O9$^{\#6}$	0.90	2.27	3.17(1)	179
N26A–H26B···O39$^{\#7}$	0.90	2.28	3.01(1)	137
N26B–H26C···O6$^{\#6}$	0.90	2.35	3.22(1)	164
N26B–H26C···O39$^{\#7}$	0.90	2.57	3.02(1)	112
N26B–H26D···O48A$^{\#6}$	0.90	2.21	2.98(1)	143

[a]H atom has not been determined but donor and acceptor atoms have been inferred by geometrical and bond valence sum considerations. Symmetry transformations used to generate equivalent atoms: $^{\#1}$ $x-1/2, -y+2, z$; $^{\#2}$ $-x+1, -y+1, z+1/2$; $^{\#3}$ $x-1/2, -y+1, z$; $^{\#4}$ $-x+3/2, y, z-1/2$; $^{\#5}$ $-x+1, -y+1, z-1/2$; $^{\#6}$ $-x+1/2, y, z+1/2$; $^{\#7}$ $-x+1, -y+2, z+1/2$; $^{\#8}$ $x+1/2, -y+2, z$; and $^{\#9}$ $-x+1/2, y, z-1/2$.

Thus, with increase of temperature an ordered phase, **II**, of lower density ($\rho_{calc} = 2.185\,Mg\,m^{-3}$, $T = 298\,K$ [5]) is dehydrated and transforms into a disordered phase, **I**, of higher density ($\rho_{calc} = 2.307\,Mg\,m^{-3}$, $T = 298\,K$). The ZnPO frameworks of **I** and **II** are topologically different, and during interconversion not only loss or uptake of water molecules takes place but also hydrolytic cleavage and reformation of Zn–O–P linkages between pillars and layers as well as within the layers themselves. Such reconstructive phase transformations are likely to involve under hydrothermal conditions at least partial dissolution of the solids. This needs, however, verification by in situ studies employing methods with higher time resolution (e.g., synchrotron XRD) as compared to our laboratory XRD methods.

There are only few recent papers that also report on the reversibility of the transformation of amine-containing metal phosphates in solid–solvent systems. For some ZnPOs of varying dimensionality [26] and for two 1D aluminophosphates with different tetrahedral chains [33], reversible interconversion has been achieved by change of pH. We have described elsewhere [34] the thermally induced reversible transformation of two 3D ZnPO polymorphs. Such knowledge about the

reversibility of phase transformations is of significance for better understanding of and future investigations into phase formation processes [26,35].

Finally, we mention that one of the first open-framework ZnPOs ever prepared in the presence of an organic amine, denoted ZnPO/dab-A (dab = 1,4-diazabicyclo[2.2.2]octane) by Harrison et al. [36], is structurally closely related to **I** and **II**, in possessing the same kind of (4.8^2 net) layers and HPO_4 pillars, but with differences in the distortion of the layers and the stacking of layers.

Acknowledgments

The authors are grateful to B. Beiße for performing TG/DTA measurements.

References

[1] Ch. Baerlocher, W.M. Meier, D.H. Olson, Atlas of Zeolite Framework Types, fifth revised edition, Elsevier, Amsterdam, 2001, http://www.iza-structure.org/databases.
[2] T.E. Gier, G.D. Stucky, Nature 349 (1991) 508.
[3] W.T.A. Harrison, T.E. Gier, K.L. Moran, J.M. Nicol, H. Eckert, G.D. Stucky, Chem. Mater. 3 (1991) 27.
[4] A. Simon-Masseron, J.-L. Paillaud, J. Patarin, Chem. Mater. 15 (2003) 1000.
[5] S. Natarajan, Inorg. Chem. 41 (2002) 5530.
[6] A.K. Cheetham, G. Férey, T. Loiseau, Angew. Chem., Int. Ed. Engl. 38 (1999) 3268.
[7] M.E. Davis, Nature 417 (2002) 813.
[8] G. Schulz-Ekloff, D. Wöhrle, B. van Duffel, R.A. Schoonheydt, Mircopor. Mesopor. Mater. 51 (2002) 91.
[9] Y. Wang, J. Yu, M. Guo, R. Xu, Angew. Chem., Int. Ed. Engl. 42 (2003) 4089.
[10] W.T.A. Harrison, R.W. Broach, R.A. Bedard, T.E. Gier, X. Bu, G.D. Stucky, Chem. Mater. 8 (1996) 691.
[11] R.M. Yates, W.T.A. Harrison, J. Mater. Chem. 12 (2002) 1103.
[12] M. Eddaoudi, J. Kim, N. Rosi, D. Vodak, J. Wachter, M. O'Keeffe, O.M. Yaghi, Science 295 (2002) 469.
[13] R.J. Francis, D. O'Hare, J. Chem. Soc., Dalton Trans. (1998) 3133.
[14] G. Férey, J. Fluorine Chem. 72 (1995) 187.
[15] S. Oliver, A. Kuperman, G.A. Ozin, Angew. Chem., Int. Ed. Engl. 37 (1998) 46.
[16] C.N.R. Rao, S. Natarajan, A. Choudhury, S. Neeraj, A.A. Ayi, Acc. Chem. Res. 24 (2001) 80.
[17] A.A. Ayi, A. Choudhury, S. Natarajan, S. Neeraj, C.N.R. Rao, J. Mater. Chem. 11 (2001) 1181.
[18] A. Choudhury, S. Neeraj, S. Natarajan, C.N.R. Rao, J. Mater. Chem. 11 (2001) 1537.
[19] A. Choudhury, S. Neeraj, S. Natarajan, C.N.R. Rao, J. Mater. Chem. 12 (2002) 1044.
[20] S. Natarajan, Chem. Commun. (2002) 780.
[21] M. Dan, D. Udayakumar, C.N.R. Rao, Chem. Commun. (2003) 2212.
[22] A.C. Christensen, A. Bareges, R.B. Nielson, R.G. Hazell, P. Norby, J.C. Hanson, J. Chem. Soc., Dalton Trans. (2001) 1611.
[23] R.I. Walton, A.J. Norquist, S. Neeraj, S. Natarajan, C.N.R. Rao, D. O'Hare, Chem. Commun. (2001) 1990.
[24] R.I. Walton, A. Norquist, R.I. Smith, D. O'Hare, Faraday Discuss. 122 (2002) 331.
[25] S. Natarajan, L. van Wüllen, W. Klein, M. Jansen, Inorg. Chem. 42 (2003) 6265.
[26] A. Choudhury, C.N.R. Rao, Chem. Commun. (2003) 366.
[27] R. Singh, J. Doolittle, P.K. Dutta, J. Phys. Chem. B 106 (2002) 2146.
[28] A.L. Spek, PLATON, a multipurpose crystallographic tool, Utrecht University, The Netherlands, 2001, http://www.cryst.chem.uu.nl.
[29] G.M. Sheldrick, SHELXS-86, Program for Crystal Structure Solution, Universität Göttingen, Germany, 1986.
[30] G.M. Sheldrick, SHELXL-97, Program for Crystal Structure Refinement, Universität Göttingen, Germany, 1997.
[31] J.V. Smith, Chem. Rev. 88 (1988) 149.
[32] I.D. Brown, D. Altermatt, Acta Crystallogr. B 41 (1985) 244.
[33] K. Wang, J. Yu, C. Li, R. Xu, Inorg. Chem. 42 (2003) 4597.
[34] M. Wiebcke, B. Marler, Solid State Sci. 6 (2004) 213.
[35] F. Millange, R.I. Walton, N. Guillou, T. Loiseau, D. O'Hare, G. Férey, Chem. Mater. 14 (2002) 4448.
[36] W.T.A. Harrison, T.E. Martin, T.E. Gier, G.D. Stucky, J. Mater. Chem. 2 (1992) 175.